

ICD-LM: Configuring Vision-Language In-Context Demonstrations by Language Modeling

Yingzhe Peng¹ Xu Yang^{1*} Haoxuan Ma¹ Shuo Xu¹ Chi Zhang²
Yucheng Han³ Hanwang Zhang³

¹ Key Laboratory of New Generation Artificial Intelligence Technology & Its Interdisciplinary Applications, (Southeast University), Ministry of Education

² Tencent

³ Nanyang Technological University

yingzhhe.peng@seu.edu.cn, xuyang_palm@seu.edu.cn, haoxuan-ma@seu.edu.cn, xushuo@seu.edu.cn, johczhang@tencent.com, yucheng002@e.ntu.edu.sg, hanwangzhang@ntu.edu.sg

Abstract

This paper studies how to configure powerful In-Context Demonstration (ICD) sequences for a Large Vision-Language Model (LVLM) to solve Vision-Language tasks through In-Context Learning (ICL). After observing that configuring an ICD sequence is a mirror process of composing a sentence, i.e., just as a sentence can be composed word by word via a Language Model, an ICD sequence can also be configured one by one. Consequently, we introduce an ICD Language Model (ICD-LM) specifically designed to generate effective ICD sequences. This involves creating a dataset of hand-crafted ICD sequences for various query samples and using it to train the ICD-LM. Our approach, diverging from traditional methods in NLP that select and order ICDs separately, enables to simultaneously learn how to select and order ICDs, enhancing the effect of the sequences. Moreover, during data construction, we use the LVLM intended for ICL implementation to validate the strength of each ICD sequence, resulting in a model-specific dataset and the ICD-LM trained by this dataset is also model-specific. We validate our methodology through experiments in Visual Question Answering and Image Captioning, confirming the viability of using a Language Model for ICD configuration. Our comprehensive ablation studies further explore the impact of various dataset construction and ICD-LM development settings on the outcomes. The code is given in <https://github.com/ForJadeForest/ICD-LM>.

1. Introduction

With the escalation in model size [4, 6, 7, 32, 44, 45], the capabilities of Large Language Models (LLMs) have been largely enhanced. One salient emerging ability is In-Context Learning (ICL) [8, 38, 39], which can make LLMs quickly adapt to novel tasks using a few examples that are termed In-Context Demonstrations (ICDs). Crucially, ICL does not need gradient updates to model parameters, thereby circumventing challenges tied to additional data collection and model fine-tuning. Inspired by such success in NLP, researchers in the Vision-Language (VL) domain also design Large Vision-Language Models (LVLMs) capable of ICL [1, 2, 33, 47], paving the way for novel research and applications. Then an elemental question arising from these trained LVLMs is how to achieve optimal ICL performance across various vision-language tasks. Before delving into ICL performance optimization in VL, we first retrospect the studies on ICL in NLP. While well-trained LLMs are identified as good In-Context Learners [4, 21], it has been observed that diverse ICD configurations heavily affect the ICL performance. For example, using different examples from the supporting set as ICDs [9, 18, 23], or even changing the orders of these ICDs [11, 20, 48], may lead to significant performance fluctuations. Driven by these findings, researchers design diverse heuristic-based (e.g., embedding similarity-based) retrieval methods [18, 28, 30] to select representative examples as the ICDs. Then these ICDs are reordered based on some principles, e.g., the Minimal Description Length [40] or Global and Local Entropy [20], for further improving the results.

While employing these methods to configure the ICDs yields consistent improvements, they still suffer from a few limitations. First, the independent operation of retrieval and

*Corresponding author.

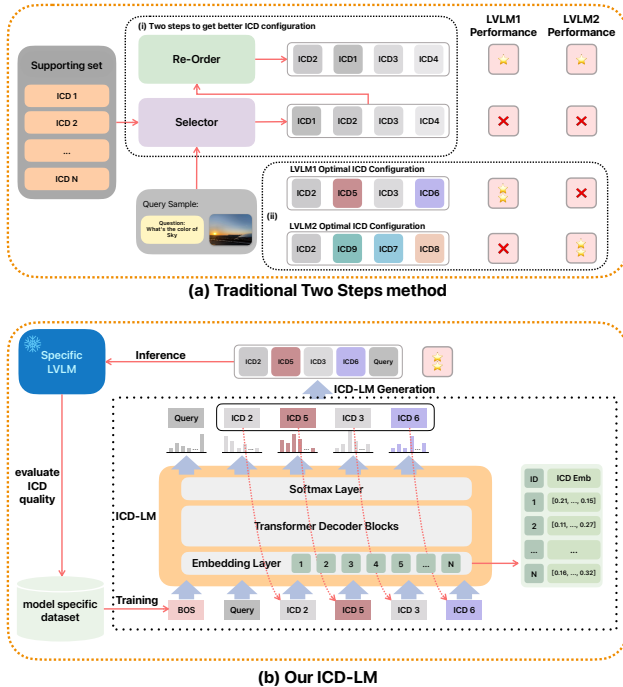


Figure 1. (a) The traditional ICD configuration methods separately select and order the ICDs, leading to sub-optimal ICL performance. (b) Our ICD-LM enables the step-by-step generation of ICD configurations and simultaneously considers the selection of ICDs and the ordering of ICD sequences.

reordering processes potentially yields sub-optimal results. For example, using similarity-based retrieval methods followed by reordering of ICD configuration may lead to the sub-optimal ICL performance, as shown in Fig. 1 (a) (i), where colors closer to the query sample (grey) in the figure indicate higher similarity. Second, as shown in Fig. 1 (a) (ii), researchers have noted that different LLMs exhibit sensitivities to particular ICD configurations [20], suggesting that the ICD configuration should be model-specific. Yet, most retrieval or reordering strategies remain model-agnostic, potentially leading to sub-optimal results.

Then if we want to directly extend these NLP strategies to VL, the above-mentioned challenges will be further exacerbated by the multimodal combinatorial complexity of vision and language data. For instance, although retrieving similar text samples typically yields favorable results in NLP, simply retrieving similar single-modal data, such as images, may not guarantee the best performance in VL tasks [41]. However, attempting to match both visual and textual modalities during retrieval will further magnify the time complexity. Additionally, VL tasks have more diverse problem structures than NLP, necessitating distinct retrieval or reordering strategies tailored to each VL task, thereby elevating the design and labor overhead.

In this study, we address these issues by introducing a

novel approach for configuring ICDs to solve diverse VL tasks. Before delving into our approach, we reconsider the ideal process of constructing an ICD sequence. Given the query sample, we hope to subsequently select a series of ICDs that can maximize the ICL performance. This iterative selection mirrors the construction of a sentence wherein the word is selected one by one to ensure fluency. Recognizing this analogy, we propose to treat the ICD configuration as a specialized Language Model (LM). The only difference is that the vocabulary of this ICD-LM is not conventional words, but are the examples from the supporting set that will be used as ICDs.

We show the ICD-LM pipeline in Fig. 1 (b). To deploy this ICD-LM, a primary challenge arises that we do not have a "ground-truth" dataset that indicates which examples or their orders can form an optimal ICD sequence for a specific LVLM-based in-context learner. To address it, we construct a dataset containing the pairs of a query and the corresponding ICD sequence. During construction, we use this frozen specific LVLM to measure whether an ICD sequence is good for the query or not. In this way, the constructed dataset becomes model-specific. Then we use this dataset to train a Transformer-based ICD-LM where each token in the vocabulary represents an example from the supporting set. During training, the ICD-LM concurrently learns the selection and ordering of ICDs, eliminating the necessity to operate two separate stages for constructing an ICD sequence as previous methods.

Besides alleviating the above-mentioned limitations, we also find some other interesting characteristics of our method. First, we evaluate the length extrapolation ability of ICD-LM, which pertains to its performance when generating ICD sequences that exceed the maximum length represented in the dataset. This is contrasted with its interpolation ability, *i.e.*, the performance within the maximum ICD length of that dataset. For instance, if a dataset only contains 2-shot ICDs, the interpolation ability denotes the effect of the 1- and 2-shot ICDs when implementing ICL, while the extrapolation ability denotes the effect of more shot ICDs like 4- or even 8-shot ICDs. Interestingly, we find that the trained ICD-LM has strong length extrapolation ability, *e.g.*, when trained on a dataset containing only 2-shot ICDs, it can proficiently configure 4-shot ICDs. Second, the trained ICD-LM may configure a fixed ICD sequence for each query while achieving excellent ICL performance. For example, in the IC/VQA tasks, the golden ICD sequence achieves 6.91/1.24 improvements compared with a strong baseline that retrieves the ICDs by similar images.

2. Related Work

Models with In-Context Learning Ability. Prompt engineering enables pre-trained Large Language Mod-

els(LLMs) to address downstream tasks without the need for fine-tuning [4, 24, 29]. A variant, ICL, enhances this ability by constructing prompts with a few examples. This has been demonstrated in LLMs such as GPT-3 [4], LLaMA [32], and MPT [31]. Recently, witnessing such success in NLP, the VL domain has also developed numerous LVLMs with prompt engineering abilities [1, 13, 17, 33, 43, 49]. With the support of LLM, Frozen [33] and Flamingo [1] have developed the ability for ICL. Among these LVLMs, Flamingo simulates the ICL approach during training, resulting in a more powerful ICL ability. However, due to the unavailability of an official open-source version of Flamingo, we use an unofficial implementation, OpenFlamingo [2] in this study to explore whether ICD-LM can configure useful ICD sequences.

Configuring In-Context Demonstrations. Although ICL assists LLMs in better adapting to downstream tasks, its performance is highly sensitive to the selection [9, 18, 23] and ordering [11, 20, 48] of ICDs. Numerous studies have explored diverse methods to select ICDs in the NLP field. For example, [18] selects ICDs based on the embedding similarity between ICDs and test samples where the embeddings are extracted from an existent language encoder. Such method is further developed by training an encoder specifically for selection [5, 15, 15, 26, 36, 37, 42]. Additionally, [14, 22, 40] leverage LLM outputs to select and [46] formulates ICD selection as a Markov decision process [3].

Regarding the ordering of ICDs, researchers propose some principles to measure the quality of ICD configurations, *e.g.*, the Minimal Description Length [40] and Global and Local Entropy [20]. However, these reordering methods are limited to classification tasks in NLP, as they require the calculation of conditional probabilities for each label given the task inputs. These approaches are inapplicable to certain tasks lacking a predefined label space, such as open-ended question answering or text generation.

Besides these NLP studies, in VL, [41] explores diverse ICD configurations on image captioning, while only the heuristic-based methods are used for selecting ICDs and do not consider the ordering. In contrast, our ICD-LM can simultaneously learn how to select and reorder the samples and moreover, our ICD-LM is model-specific.

3. Model-Specific ICD-LM

In this section, we introduce how to build a model-specific ICD-LM for configuring the ICD sequence for a given LVLM. First, we briefly introduce the formulations of ICL for Vision-Language (VL) tasks in section 3.1. Then we show how to construct a model-specific dataset (section 3.2) that will be used to train the ICD-LM, whose structure will be detailed in Section 3.3.

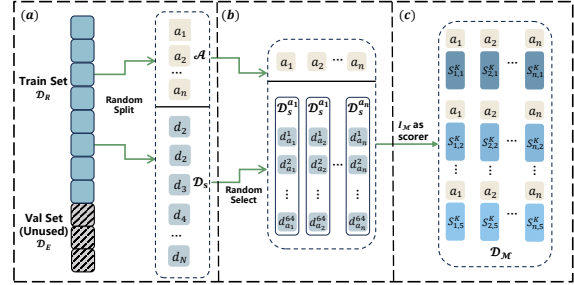


Figure 2. The pipeline of constructing \mathcal{D}_M . The darker color of $S_{i,j}^K$ indicates a higher score given by Eq. 2 in figure (c).

3.1. In-Context Learning (ICL)

Given a query input x' , ICL predicts the corresponding output y' using a well-trained foundation model \mathcal{M} , conditioned on the concatenation of an in-context sequence \mathcal{S} and this query. If the in-context sequence contains K -shot ICDs, it is denoted as: $\mathcal{S}^K = \{\hat{d}_1, \hat{d}_2, \dots, \hat{d}_K\}$, where \hat{d}_k is the k -th ICD. Then ICL can be formulated as:

$$y' \leftarrow P_{\mathcal{M}}(y' | \mathcal{S}^k, x'), \quad (1)$$

where $P_{\mathcal{M}}$ denotes the predicted probability of \mathcal{M} and “ \leftarrow ” represents the decoding strategy, *e.g.*, beam search.

For each ICD \hat{d} , it is selected from a supporting dataset $\mathcal{D}_S = \{d_1, \dots, d_N\}$, where each sample $d_i = (x_i, y_i)$: x_i and y_i respectively denote the input and the corresponding label. It is noteworthy that in diverse VL tasks, x and y have different forms. For instance, in Image Captioning (IC), x is the image and y is the caption; and in Vision Question Answering (VQA), x contains the image and the question, while y is the answer.

3.2. Constructing the Model-Specific Dataset

To train our model-specific ICD-LM for generating effective ICD sequences for a given LVLM \mathcal{M} , we should first construct a model-specific dataset \mathcal{D}_M containing high-quality ICD sequences for different query inputs. To avoid confusion, Figure 2 shows how to construct \mathcal{D}_M from an VL dataset, *e.g.*, the COCO dataset [16] for IC. Formally, given an dataset \mathcal{D} which is already split into the training part \mathcal{D}_R and the test part \mathcal{D}_E , we build \mathcal{D}_M only from the training part \mathcal{D}_R .

As shown in Fig. 2 (a), initially, we randomly select n samples from \mathcal{D}_R to form an anchor set \mathcal{A} . Then for each sample $a_m = \{x_m, y_m\} \in \mathcal{A}$, we aim to construct a K -shot in-context sequence \mathcal{S}_m^K for it. Then $\mathcal{D}_M = \{(a_1, \mathcal{S}_1^K), (a_2, \mathcal{S}_2^K), \dots, (a_M, \mathcal{S}_M^K)\}$ where each training sample contains an query a_m and the corresponding K -shot in-context sequence \mathcal{S}_m^K .

To avoid confusion, we remove the subscript m in following. To construct $\mathcal{S}^K = \{d_1, \dots, d_K\}$, we need to select K -shot samples from the supporting set \mathcal{D}_S , which is set to the complement set of \mathcal{A} in \mathcal{D}_R : $\mathcal{D}_R \setminus \mathcal{A}$. Meantime, we also

need to decide which samples should be selected in turn. To achieve this, given the anchor sample $\mathbf{a} = \{\mathbf{x}, \mathbf{y}\}$ and the partially constructed in-context sequence, *e.g.*, a $k - 1$ -shot \mathcal{S}^{k-1} , we need to know that after adding which sample $\mathbf{d} \in \mathcal{D}_S$, the ICL performance improvement can be maximized by applying the given LVLM \mathcal{M} :

$$\hat{\mathbf{d}}_k = \arg \max_{\mathbf{d} \in \mathcal{D}_S} I_{\mathcal{M}}(\{\mathbf{d}, \mathcal{S}^{k-1}\}, \mathbf{a}) - I_{\mathcal{M}}(\mathcal{S}^{k-1}, \mathbf{a}), \quad (2)$$

where $I_{\mathcal{M}}$ is one kind of ICL performance measurement related to \mathcal{M} . Note that Eq. (2) actually uses the greedy sampling method to select the samples every time, while we can use beam search here to further achieve a better solution. Additionally, to improve the diversity of the dataset, we will keep the top- b highest-scoring ICD sequences $\{S_{m,1}^K, S_{m,2}^K, \dots, S_{m,b}^K\}$ at the last iteration for each a_m , where b is equal to the beam size. For example, when setting beam size to 5 as shown in Fig. 2 (c), we can get 5 diverse high-quality ICD sequences for an anchor sample.

Intuitively, for diverse tasks, we can use the corresponding ‘‘golden measurement’’ as $I_{\mathcal{M}}$, *e.g.*, setting it to CIDEr [35] for IC and accuracy for VQA. However, this strategy encounters two limitations. The first one is that for diverse VL tasks, we need diverse corresponding measurements, which is inconvenient. Second, some ‘‘golden measurements’’ may be impractical to deploy. For example, for IC, calculating CIDEr requires the LVLM to forward multiple times to sample an integral sentence, and then it costs expensive time burdens to construct the dataset. While for VQA, accuracy is a binary value (accuracy=1 when correct and 0 when wrong), then maybe lots of candidates in \mathcal{D}_S will make the accuracy change from 0 to 1 and then it is hard to judge which one of them is the most suitable one.

To overcome these two limitations, we use a relatively general measurement as $I_{\mathcal{M}}$. Formally, since we have the ground-truth results \mathbf{y} of the anchor sample, we can use the given LVLM \mathcal{M} to measure the prediction confidence of \mathbf{y} given the input \mathbf{x} and the in-context sequence \mathcal{S}^K :

$$\begin{aligned} I_{\mathcal{M}}(\mathcal{S}^K, \mathbf{a}) &= P_{\mathcal{M}}(\mathbf{y}|\mathcal{S}^K, \mathbf{x}) \\ &= \prod_t P_{\mathcal{M}}(y^{(t)}|\mathcal{S}^K, \mathbf{x}, y^{(1:t-1)}). \end{aligned} \quad (3)$$

Note that in VL tasks, the ground-truth label $\mathbf{y} = \{y^{(1)}, \dots, y^{(T)}\}$ is usually a text sequence, thus we can decompose the probability distribution into a series of productions. In this way, Eq. (2) selects a sample that can further maximize the prediction confidence given the query input and the current in-context sequence.

In implementation, \mathcal{D}_S usually contains huge amounts of samples, *e.g.*, \mathcal{D}_S in COCO [16] contains about 10^5 samples. However, we need to calculate Eq. (2) for each $\mathbf{d} \in \mathcal{D}_S$ when selecting $\hat{\mathbf{d}}_k$ for each $\mathbf{a} \in \mathcal{A}$, which means the whole process of building $\mathcal{D}_{\mathcal{M}}$ is quite time-consuming.

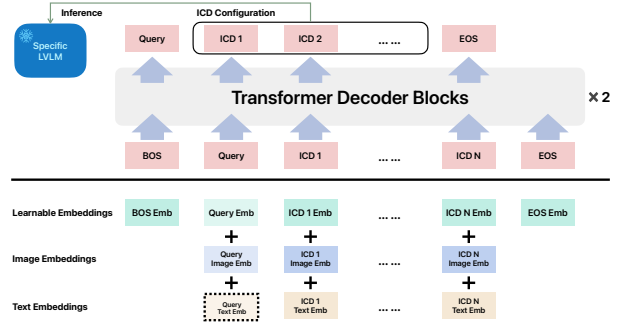


Figure 3. Top: The architecture of ICD-LM, which is a two-layer Transformer decoder blocks. Bottom: The components of the input embeddings, which is the sum of the random initialized learnable embeddings, the image and text embeddings extracted by CLIP. The dotted block means that some tasks do not exist the text input, *e.g.*, IC.

To alleviate the cost, as shown in Fig. 2 (b), for each specific \mathbf{a} , we narrow the set size by sampling a much smaller subset \mathcal{D}_S^a , *e.g.*, containing 64 samples $\mathcal{D}_S^a = \{d_a^1, d_a^2, \dots, d_a^{64}\}$, from \mathcal{D}_S for selecting $\hat{\mathbf{d}}_k$. We use diverse sampling strategies to construct this subset, *e.g.*, retrieving some similar samples as \mathbf{a} , and implement exhaustive ablation studies to explore which strategies are useful in Section 4.4.

3.3. Training Model-Specific ICD-LM

After constructing the model-specific dataset $\mathcal{D}_{\mathcal{M}}$, we use it to train our ICD-LM, as Figure 3 shows, it is a two-layer Transformer decoder blocks [34]. The primary difference between our ICD-LM and the traditional LM lies in the tokens of the vocabulary. Specifically, the tokens in our vocabulary are the samples from the supporting set \mathcal{D}_S , *e.g.*, the first token corresponds to the first sample in \mathcal{D}_S .

In this way, given the query sample, the ICDs can be selected one by one based on the token distribution produced by the trained ICD-LM, just as when composing a sentence, the words are selected one by one from the word vocabulary. Besides the tokens from \mathcal{D}_S , three special tokens are added into the vocabulary to help configure the ICD sequence, which are [BOS], [EOS], and [QUERY], respectively representing the beginning of a sequence, the end of a sequence, and the test sample. Then given a data sample ($\mathcal{S}^K = \{\mathbf{d}_1, \dots, \mathbf{d}_K\}, \mathbf{x}'$) from $\mathcal{D}_{\mathcal{M}}$ where \mathcal{S}^K is the ICD sequence and \mathbf{x}' is the query input, we reformulate it into $\{[\text{BOS}], [\text{QUERY}] + \mathbf{x}', \mathbf{d}_1, \dots, \mathbf{d}_K, [\text{EOS}]\}$ where $[\text{QUERY}] + \mathbf{x}'$ denotes to add two embeddings. This reformulated sequence is input into the ICD-LM for training.

To train the ICD-LM, we first need to embed the tokens of the vocabulary to get dense embeddings. Since each token contains both image and text, we use the vision encoder $F_I(\cdot)$ and the language encoder $F_T(\cdot)$ of CLIP [25] to em-

bed the image and text, respectively. Meanwhile, we add each of these embeddings with a learnable part which is randomly initialized. Then for the i -th token $d_i = (I_i, T_i)$ in the vocabulary where I_i and T_i are the corresponding image and text, respectively, its token embedding is e_i :

$$e_i = F_I(I_i) + F_T(T_i) + r_i, \quad (4)$$

where r_i is the randomly initialized learnable embedding for the i -th token. Note that T_i varies between IC and VQA tasks. In IC, T_i represents the caption, whereas in VQA, it denotes the question and the answer.

For the test query x' , we also use the same vision and language encoders to embed it. For VQA, the image and question will be embedded and summed, while for IC, only the image is embedded. Lastly, we employ the cross-entropy loss for training as a standard LM that given the previously $k - 1$ tokens, we maximize the probability of the k -th ground-truth token.

3.4. Configuring the ICD Sequence

After training the ICD-LM, we use it to configure the ICD sequence. Given a query sample x' , we initialize the input sequence as $\{[\text{BOS}], [\text{QUERY}] + x'\}$ and then generate the ICDs one by one. After iteratively sampling K -shot ICDs, we can compose the corresponding in-context sequence for x' and then use Eq. (1) to implement the ICL.

4. Experiments

4.1. Tasks and Datasets

Our approach is evaluated on MS-COCO for Image Captioning (IC) and VQAV2 for Visual Question Answering (VQA). For each corresponding dataset, we use the train split to construct the \mathcal{D}_M for training ICD-LM and use the validation split to evaluate the performance of ICD configurations generated by ICD-LM.

MS-COCO [16]: MS-COCO is widely used in IC, which is divided into 118, 287 training, 5, 000 validation, and 5, 000 test image-caption pairs. Notably, each training image is associated with five distinct human-annotated captions.

VQAV2 [10]: VQAV2 emphasizes open-ended VQA tasks, which encompasses 4, 437, 570 question-answer pairs in its training split, supplemented by an additional 2, 143, 540 pairs in the validation split.

4.2. Implementation Details

Constructing \mathcal{D}_M : We construct 2-shot \mathcal{D}_M for main experiments. We select 5000 samples to get the anchor set \mathcal{A} . For each anchor sample, we randomly choose 64 samples to build the sub-supporting set \mathcal{D}_S^a . The beam size for these processes is 5. More details are in Appendix.

Training ICD-LM: Different training strategies are employed for IC and VQA when training ICD-LM. In IC, the weight of CLIP model will be frozen, and an MLP adapter is

Table 1. Prompt Formats for IC and VQA tasks with placeholders.

Task	Prompt Format
VQA	<image>Question:<Q> Short answer:<A>
Caption	<image>Output:<X>

introduced to its output. While, for VQA, the CLIP encoder remains trainable, and no adapter is appended. Both the ICD-LM for VQA and IC use 2-layer Transformer decoder blocks [34] or LSTM [27] as the architecture of LM. The training phase leverages the AdamW optimizer [19] and a cosine learning rate scheduler. We set the learning rate to 1×10^{-4} and the batch size to 128. We train our ICD-LM for 20 epochs. All training processes are carried out with mixed precision and 2 RTX3090 GPUs.

Implementing ICL: To implement ICL, we use OpenFlamingoV2-9B [2] as our LVLm. We use beam search during inference where the beam size is set to 3. Besides, we set the maximum number of generated tokens as 20 in IC and 5 in VQA. All experiments are deployed on an RTX 3090, operating in BF16 mode. The prompt structures of IC and VQA are shown in Table 1.

4.3. Results and Analyses

4.3.1 Comparison Methods

We compare ICD-LM to 4 ICD selection strategies:

Random Sample (RS): RS constructs \mathcal{S}^k by randomly selecting and ordering k ICDs from \mathcal{D}_S .

Similarity-based Retrieval methods: These methods form \mathcal{S}^k by computing the similarity between the query input x' and ICDs in \mathcal{D}_S . Specifically, we use CLIP to extract the features of text or image and use cosine similarity to measure the similarity between the extracted features. We follow [18], sorting examples in ascending order by their similarity to the query input, so the rightmost demonstration is the closest example. (1). **Similarity-based Image-Image Retrieval (SIIR):** We select k ICDs from \mathcal{D}_S with highest image similarity to the query image. (2). **Similarity-based Text-Text Retrieval (STTR):** We select k ICDs from \mathcal{D}_S that have most similar texts to the text of the query. For VQA, with question as input, we can use STTR to form \mathcal{S}^k . While for IC, the query input is only an image without any text input, thus STTR is infeasible. (3). **Similarity-based Image-Text Retrieval (SITR):** Taking advantage of the cross-modal retrieval capability of CLIP, we can compute the similarity between different modalities. Specifically, we compute the similarity between query image and all text of $d_i \in \mathcal{D}_S$ and select ICDs whose texts have the top- k similarities with the query image. The text input varies per task, e.g., it is the caption for IC and the question for VQA.

4.3.2 Main Result

The results for various ICD selection strategies are summarized in Table 2 for IC and VQA. Due to the significant increase in inference time with a higher number of shots, we only tested the inference results for 6-shot and 8-shot configurations. In the tables, we respectively show the length interpolation and extrapolation abilities of ICD-LM. Specifically, interpolation/extrapolation respectively mean that the performance of the generated ICDs whose length is smaller/larger than the length of the ICD sequence in \mathcal{D}_M . Since \mathcal{D}_M only contains 2-shot ICDs, the interpolation/extrapolation abilities are respectively represented by “Avg:1~2”/“Avg:3~8”, where “Avg:1~2” denotes the average score over using 1-and 2-shot ICDs during ICL and “Avg:3~8”/“Avg:1~8”^{*} has the similar meaning. For “Avg:1~8”, it shows the comprehensive performance. In order to eliminate any potential bias in each method, the following analysis will mainly compare the Avg: $i\sim j$.

Overall, ICD-LM achieves the best performance on most cases compared to other methods. Notably, ICD-LM consistently outperforms other methods for the Avg:1~2. Specifically, in IC, ICD-LM surpasses the best similarity-based retrieval method, SIIR, by 6.03 in CIDEr score (84.32 vs. 78.29). Similarly, for VQA, ICD-LM exceeds the performance of the best similarity-based retrieval method, STTR, by achieving an accuracy 3.07 higher (48.75 vs. 45.68). The results indicate that ICD-LM performs well in generating 2-shot ICD configurations.

Moreover, we find that ICD-LM has remarkable extrapolation abilities. Regarding the Avg:3~8 metric, ICD-LM maintains the top performance in both IC and VQA. Specially, compared with SIIR, ICD-LM achieves 0.8 higher CIDEr in IC (96.52 vs. 95.72) and 0.75 higher accuracy in VQA (52.59 vs. 51.84). Thus, even with a dataset consisting of only 2 shots, ICD-LM is still able to generate longer high-quality ICD configurations. These experiment results indicate that ICD-LM can effectively generate optimal ICD configurations, thereby assisting LVLM in predictions.

Furthermore, we observe the ICD configurations generated by ICD-LM are more robust. We can observe the SITR underperforms when compared to RS in both IC and VQA.

For STTR in VQA, it exhibits a performance decline compared to RS when the number of shots is relatively large. For instance, it lags behind RS by 0.81 in the 8-shot configuration. These results highlight that not all similarity-based retrieval methods are effective in different multi-modal tasks.

In Fig. 4, we visualize several ICD configurations and observe that, when the context of the ICDs is similar to query sample, OpenFlamingo tends to excessively rely on text information of ICDs when predicting labels. For exam-

Table 2. Results of diverse ICL methods on IC and VQA.

		Interpolation			Extrapolation					Avg:1~8
		Shot 1	Shot 2	Avg:1~2	Shot 3	Shot 4	Shot 6	Shot 8	Avg:3~8	
IC	RS	73.32	82.95	78.14	87.72	93.65	95.81	97.42	93.65	88.48
	SITR	66.05	77.69	71.87	83.46	85.05	89.84	93.57	87.98	82.61
	SIIR	71.71	84.87	78.29	90.83	93.22	97.80	101.01	95.72	89.91
	ICD-LM	80.02	88.63	84.32	93.41	96.06	97.26	99.35	96.52	92.45
VQA	RS	41.97	45.92	43.95	48.17	48.95	51.18	51.44	49.94	47.94
	SITR	40.17	43.58	41.88	46.03	47.5	49.72	50.75	48.50	46.29
	SIIR	43.31	47.46	45.39	49.85	50.68	53.23	53.58	51.84	49.69
	STTR	44.6	46.75	45.68	47.92	49.05	50.06	49.47	49.13	47.98
	ICD-LM	46.66	50.83	48.75	51.91	52.15	53.29	53.01	52.59	51.31

ple, in Fig. 4 (a) and (b), all the ICD questions are yes-or-no type, which causes LVLMs to output “no” even when faced with a “What” type question of the query sample. While for IC in Fig. 4 (c) and (d), SITR incorrectly outputs “London” even though the location is not explicitly indicated in the query image, while SIIR even leads LVLMs to directly copy the text from the ICD. This behavior, identified as Short-cut Inference, has been previously highlighted in a study [41]. Conversely, ICD-LM generates more diverse ICD configurations, thereby preventing misleading inferences.

4.4. Ablation Studies

We use ablation studies to explore the effects of diverse settings on our approach, including (1) diverse \mathcal{D}_M configurations; (2) diverse scorers I_M in Eq. (3); (3) diverse LM structures; (4) \mathcal{D}_M with longer few-shot ICDs; and (5) randomly ordering the ICD-LM generated ICD sequences.

Diverse \mathcal{D}_M Configurations. We generate 2-shot \mathcal{D}_M by different settings to investigate the corresponding effects. We select three factors for our ablation studies: beam size b ; the number n of samples in \mathcal{A} ; and the sampling method of \mathcal{D}_S^g , which includes 3 methods: **Random**: Selecting randomly from \mathcal{D}_S ; **Similar Text (Sim-T)**: Selecting the highest textual similarity sample with anchor sample a from \mathcal{D}_S ; **Similar Image (Sim-I)**: Selecting the highest visual similarity sample with anchor sample a from \mathcal{D}_S .

Table 3 & 4 show the results for different \mathcal{D}_M configurations on IC and VQA, respectively. We find that ICD-LM can consistently improve the performance compared with the baseline RS[†] in Avg:1~2. As for length extrapolation capability, only *Sim-T* gets a lower score than RS. These comparisons confirm the robustness of our method.

Besides, we observe that increasing the beam size has a positive correlation with ICD-LM performance. Specifically, as the beam size increases from 1 to 5, the CIDEr score increases by 2.79 for IC and the accuracy increases 1.73 in VQA in Avg:1~8. This suggests that a diverse \mathcal{D}_M encompasses a broader range of high-quality ICD configurations, which can help train a better ICD-LM. However, an excessively large beam size can negatively impact performance. For instance, in VQA, the accuracy of $b = 10$ decays 0.12 than $b = 5$ in Avg:1~8. We hypothesize this drop in performance is due to the introduction of lower-scoring

^{*}Not concluding 5-shot and 7-shot.

[†]The RS means Random Sample ICD retrieval method which is mentioned in Section 4.3.1.

Table 3. CIDEr of diverse \mathcal{D}_M configurations on IC.

	Interpolation			Extrapolation					Avg:1~8
	Shot 1	Shot 2	Avg:1~2	Shot 3	Shot 4	Shot 6	Shot 8	Avg:3~8	
RS	73.32	82.95	78.1	87.72	93.65	95.81	97.42	93.6	88.5
$b = 1$	75.67	84.15	79.91	90.10	92.93	95.92	99.16	94.53	89.66
$b = 5$	80.02	88.63	84.32	93.41	96.06	97.26	99.35	96.52	92.45
$b = 10$	80.64	89.27	84.96	94.47	96.26	98.58	99.15	97.12	93.06
$n = 1000$	79.55	88.34	83.94	91.16	96.25	99.70	99.87	96.74	92.48
$n = 3000$	79.30	88.96	84.13	93.28	97.66	99.34	100.15	97.60	93.11
$n = 5000$	80.02	88.63	84.32	93.41	96.06	97.26	99.35	96.52	92.45
Sim-I	75.32	88.61	81.96	93.28	95.28	97.71	98.19	96.11	91.40
Sim-T	75.78	86.66	81.22	84.39	84.27	88.47	93.53	87.66	85.52
Random	80.02	88.63	84.32	93.41	96.06	97.26	99.35	96.52	92.45

Table 4. Accuracy of diverse \mathcal{D}_M configurations on VQA.

	Interpolation			Extrapolation					Avg:1~8
	Shot 1	Shot 2	Avg:1~2	Shot 3	Shot 4	Shot 6	Shot 8	Avg:3~8	
RS	41.97	45.92	43.95	48.17	48.95	51.18	51.44	49.94	47.94
$b = 1$	44.56	48.38	46.47	49.76	49.95	52.27	52.54	51.13	49.58
$b = 5$	46.66	50.83	48.75	51.91	52.15	53.29	53.01	52.59	51.31
$b = 10$	46.89	50.27	48.58	51.54	52.17	53.00	53.26	52.49	51.19
$n = 1000$	44.66	46.12	45.39	47.96	50.15	52.09	51.56	50.44	48.76
$n = 3000$	46.04	49.08	47.56	50.42	50.88	51.54	51.59	51.11	49.93
$n = 5000$	46.66	50.83	48.75	51.91	52.15	53.29	53.01	52.59	51.31
Sim-I	45.00	49.19	47.10	50.49	51.38	52.64	52.66	51.79	50.23
Sim-T	44.30	46.45	45.38	48.36	48.95	50.46	50.44	49.55	48.16
Random	46.66	50.83	48.75	51.91	52.15	53.29	53.01	52.59	51.31

Table 5. CIDEr of diverse scorers on IC.

	Interpolation			Extrapolation					Avg:1~8
	Shot 1	Shot 2	Avg:1~2	Shot 3	Shot 4	Shot 6	Shot 8	Avg:3~8	
RS	73.32	82.95	78.14	87.72	93.65	95.81	97.42	93.65	88.48
Confidence	80.02	88.63	84.32	93.41	96.06	97.26	99.35	96.52	92.45
CIDEr	84.86	90.99	87.93	92.53	94.25	94.98	92.31	93.52	91.65

ICD sequences with a large beam size, potentially misleading ICD-LM during training.

Moreover, we observe that using more anchor samples can improve the interpolation performance in both IC and VQA, *e.g.*, when n increases from 1000 to 5000, the Avg:1~2 CIDEr/accuracy of IC/VQA increases from 83.94/45.39 to 84.32/48.75. However, we find that on IC, although the interpolation performance increases when n changes from 3000 to 5000, the extrapolation performance decays, *e.g.*, Avg:3~8 decrease from 97.60 to 96.52. One possible reason is that using Eq. (3) to build \mathcal{D}_M may introduce certain in-domain bias which is beneficial for interpolation while detrimental for extrapolation on IC. Then using more such data may enhance such in-domain bias and thus damage the extrapolation.

For different sample methods of constructing the \mathcal{D}_S^a , we find *Random* is the best in both IC and VQA. We suppose this is because selecting similar ICDs with the anchor sample from \mathcal{D}_S will damage the diversity. Previous study [12] in NLP validates that the diversity of the ICD sequences will also help improve the performance of LLMs.

Diverse Scorers I_M for evaluating ICD sequences. To evaluate the quality of ICD configurations, we can also utilize task-specific metrics as I_M to build \mathcal{D}_M , such as the CIDEr metric in IC. Table 5 compares the results obtained by using prediction confidence and CIDEr as I_M .

We can observe that the ICD-LM trained with \mathcal{D}_M using CIDEr scorer can achieve 3.61 higher than Confidence scorer in Avg:1~2, which means that the CIDEr scorer can

Table 6. Results of diverse LM structures on IC and VQA.

		Interpolation			Extrapolation					Avg:1~8
		Shot 1	Shot 2	Avg:1~2	Shot 3	Shot 4	Shot 6	Shot 8	Avg:3~8	
IC	RS	73.32	82.95	78.14	87.72	93.65	95.81	97.42	93.65	88.48
	ICD-LM(LSTM)	79.73	88.14	83.93	92.36	96.89	96.99	98.63	96.21	92.12
	ICD-LM(Transformer)	80.02	88.63	84.32	93.41	96.06	97.26	99.35	96.52	92.45
VQA	RS	41.97	45.92	43.95	48.17	48.95	51.18	51.44	49.94	47.94
	ICD-LM(LSTM)	44.64	48.55	46.60	49.77	50.51	50.71	51.72	50.68	49.32
	ICD-LM(Transformer)	46.66	50.83	48.75	51.91	52.15	53.29	53.01	52.59	51.31

Table 7. Results of ICD-LM with 4-shot \mathcal{D}_M on IC and VQA.

		Interpolation				Extrapolation			Avg:1~8	
		Shot 1	Shot 2	Shot 3	Shot 4	Avg:1~4	Shot 6	Shot 8		Avg:6~8
IC	RS	73.32	82.95	87.72	93.65	84.41	95.81	97.42	96.62	88.48
	STTR	66.05	78.66	85.47	86.47	79.16	92.27	95.63	93.95	84.09
	SHR	71.32	84.03	91.38	94.28	85.25	98.63	101.89	100.26	90.25
	ICD-LM(4-shot \mathcal{D}_M)	75.73	85.97	91.28	96.41	87.35	97.56	98.35	97.96	90.88
	ICD-LM(2-shot \mathcal{D}_M)	80.02	88.63	93.41	96.06	89.53	97.26	99.35	98.30	92.45
VQA	RS	41.97	45.92	48.17	48.95	46.25	51.18	51.44	51.31	47.94
	STTR	39.84	43.60	46.12	47.34	44.23	49.54	50.49	50.02	46.16
	SHR	43.05	47.25	49.68	50.63	47.65	53.16	53.28	53.22	49.51
	STTR	43.53	46.89	48.13	48.87	46.86	49.23	49.97	49.60	47.77
	ICD-LM(4-shot \mathcal{D}_M)	44.22	48.11	49.30	51.12	48.19	52.17	52.76	52.47	49.61
ICD-LM(2-shot \mathcal{D}_M)	46.66	50.83	51.91	52.15	50.39	53.29	53.01	53.15	51.31	

Table 8. Results of Random Order of ICD-LM generated ICDs.

	2-Shot \mathcal{D}_M		4-Shot \mathcal{D}_M	
	VQA	IC	VQA	IC
Original	50.83	88.63	51.12	85.97
Random Order	50.42	88.56	50.63	85.77

Table 9. Results of Fixed Set ICD-LM on IC and VQA.

		Interpolation			Extrapolation					Avg:1~8
		Shot 1	Shot 2	Avg:1~2	Shot 3	Shot 4	Shot 6	Shot 8	Avg:3~8	
IC	RS	73.32	82.95	78.14	87.72	93.65	95.81	97.42	93.65	88.48
	SHR	71.71	84.87	78.29	90.83	93.22	97.80	101.01	95.72	89.91
	non Fixed Set	80.02	88.63	84.32	93.41	96.06	97.26	99.35	96.52	92.45
	Fixed Set-1	75.41	88.14	81.78	92.48	94.20	99.22	103.86	97.44	92.22
	Fixed Set-2	86.37	96.03	91.20	89.80	90.81	105.29	103.51	99.63	96.82
VQA	RS	41.97	45.92	43.95	48.17	48.95	51.18	51.44	49.94	47.94
	SHR	43.31	47.46	45.39	49.85	50.68	53.23	53.58	51.84	49.69
	non Fixed Set	46.66	50.83	48.75	51.91	52.15	53.29	53.01	52.59	51.31
	Fixed Set-1	44.24	51.32	47.78	50.20	51.60	54.39	53.83	52.51	50.93
	Fixed Set-2	44.24	46.40	45.32	48.38	48.41	49.16	50.23	49.05	47.80

assign a more accurate and reasonable score for ICD configurations. However, the length extrapolation capability decreases obviously, which is 3.0 lower than Confidence score in Avg:3~8. These results evidently show the robustness of Confidence scorer. Although the result shows that the task-specific metric can help the ICD-LM to improve the interpolation ability, it will cost more time and more GPU memory to construct \mathcal{D}_M . Specifically, in IC, the time cost of constructing \mathcal{D}_M is approximately 10 times of Confidence. **Diverse LM Structures.** In Table 6, we use LSTM [27] as the structure of ICD-LM to generate ICDs for IC and VQA, respectively. We can find that even when using LSTM, our method still achieves excellent performance. In IC, the overall performance improves by 3.64 (92.12 vs. 88.48) compared to the RS baseline, while in VQA, it is improved by 1.38 (49.32 vs. 47.94). However, due to the weak representation learning capability of LSTM, its performance is lower than the Transformer structure, *e.g.*, the scores decrease by 0.33 and 1.99 in IC and VQA, respectively. Overall, these results demonstrate the ability to generate high-quality ICD configurations using various LMs. This validates that employing LM for ICD configuration is a reasonable and effective approach.

Longer Few-shot \mathcal{D}_M . We further explore the perfor-

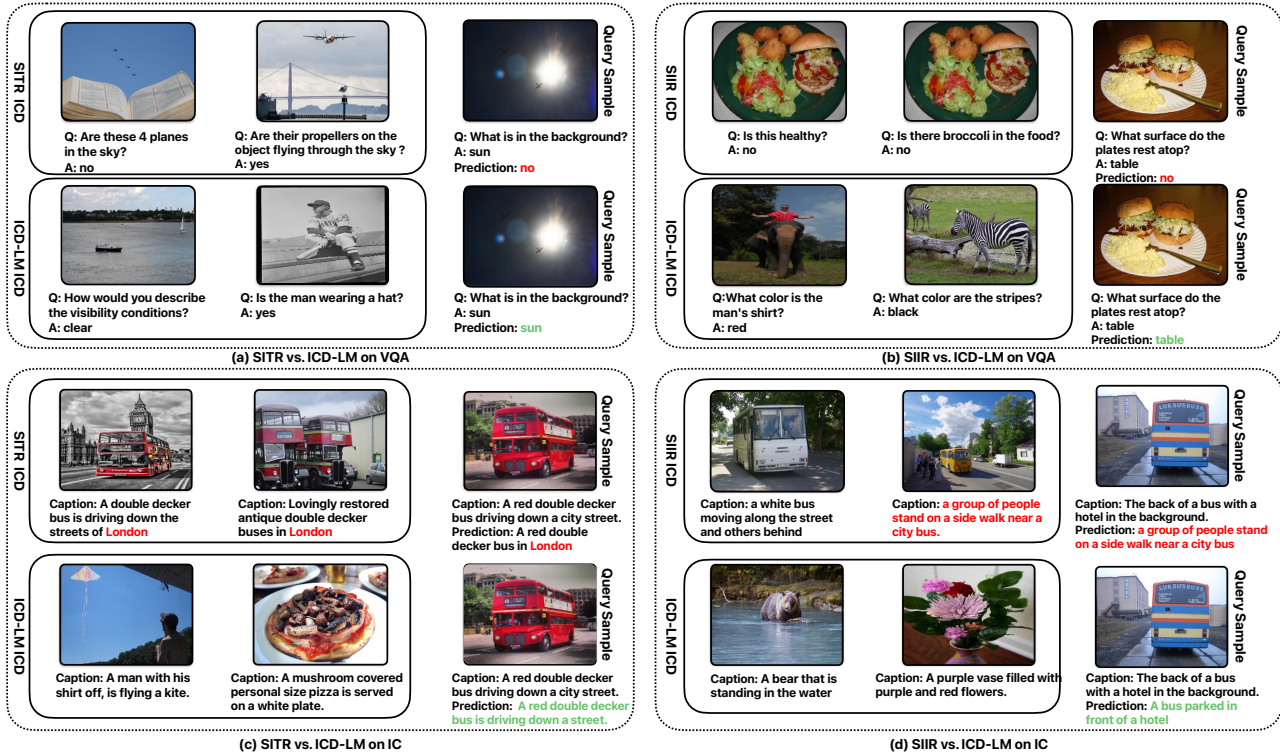


Figure 4. Visualizations of using ICDs configured by different methods on VQA. Due to the limited space, we only show the first and the last ICDs. We can find that ICD-LM tends to use more diverse ICDs and thus not lead to short-cut inference.

mance of ICD-LM using a 4-shot \mathcal{D}_M , as presented in Table 7. It is evident that ICD-LM continues to outperform other retrieval-based methods in Avg:1~8 metric.

However, we observe a notable performance reduction when the ICD-LM is trained with the 4-shot \mathcal{D}_M compared to the 2-shot \mathcal{D}_M . Specifically, for IC, there is a performance decrease of approximately 1.57 in the Avg:1~8 metric when using the 4-shot \mathcal{D}_M to train ICD-LM. We speculate that this is due to the use of Eq. (2), which may lead to becoming stuck in a local optimum when constructing longer few-shot sequences. Specifically, when selecting the k -th ICD, the previous $k-1$ ICDs are held constant. This selection process might not always result in the optimal k -shot sequence. When shot number increases, the ICD sequence may further deviate from the global optimum, leading to a decline in ICD-LM performance. Thus leading to poor performance of the ICD-LM generated by this dataset.

Random Order ICD sequence. To validate that our model achieves an effective ICD order, we randomly rearrange the ICD sequences generated by ICD-LM and evaluate the performance. Specifically, we use the ICD-LM trained with 2-shot and 4-shot \mathcal{D}_M and evaluate their performance of the 2-shot and 4-shot ICD configurations, respectively. Table 8 displays our results. It is evident that the original order of ICD configurations generated by the ICD-LM attains the

highest score in both VQA and IC, demonstrating that ICD-LM can effectively learn how to order the ICDs.

Fixed Set. During training ICD-LM, we discover that using a high learning rate and not freezing the CLIP model may make ICD-LM converge to a specific solution that for any query input, the ICD configuration is the same and we term this case “Fixed Set”. Table 9 presents the performance of multiple Fixed Set models obtained with different training parameters. The specific training parameter configurations and the generated ICD configurations will be shown in Appendix. We find that the performance of the Fixed Set models fluctuates significantly. For example, in IC, the best version, Fixed Set-2, can outperform the non-Fixed Set by 4.6 points in Avg:1~8. However, the performance of Fixed Set-2 is poorer than RS in VQA. This phenomenon of Fixed Set demonstrates that for a specific LVLM, there exists a particular ICD configuration that can universally enhance ICL capability. Therefore, we do not need to store a large number of samples for ICD retrieval; instead, we only need to use the Fixed Set samples as the core supporting set. Therefore, it is worthwhile to consider further research in the future to stabilize the performance of the Fixed Set.

5. Conclusion and Limitations

In this paper, motivated from the observation that configuring an ICD sequence is a mirror process of composing a sentence, we propose to build an ICD-LM for configuring ICDs. To achieve this, we construct a dataset containing high-quality ICD sequences to train this ICD-LM. After training, we validate the effectiveness of ICD-LM in accomplishing ICD selection and ordering by comparing it with similarity-based retrieval methods. Also, we deploy extensive ablations to validate the effectiveness of diverse settings of dataset construction and model building strategies.

One major limitation of our study is the strategy used to build $\mathcal{D}_{\mathcal{M}}$ is not optimal, which requires further improvement. This limitation is revealed by observing that the 4-shot $\mathcal{D}_{\mathcal{M}}$ performs worse than the 2-shot one, highlighting the need for a more effective approach in searching for longer ICD sequences. To address this, we plan to design function $I_{\mathcal{M}}$ to evaluate the effectiveness of ICD sequences; and use better sampling strategies in Eq. (2) to avoid the ICD sequence deviating from the global optimum.

References

- [1] Jean-Baptiste Alayrac, Jeff Donahue, Pauline Luc, Antoine Miech, Iain Barr, Yana Hasson, Karel Lenc, Arthur Mensch, Katherine Millican, Malcolm Reynolds, et al. Flamingo: a visual language model for few-shot learning. *Advances in Neural Information Processing Systems*, 35:23716–23736, 2022. 1, 3
- [2] Anas Awadalla, Irena Gao, Josh Gardner, Jack Hessel, Yusuf Hanafy, Wanrong Zhu, Kalyani Marathe, Yonatan Bitton, Samir Gadre, Shiori Sagawa, et al. Openflamingo: An open-source framework for training large autoregressive vision-language models. *arXiv preprint arXiv:2308.01390*, 2023. 1, 3, 5
- [3] Richard Bellman. A markovian decision process. *Journal of mathematics and mechanics*, pages 679–684, 1957. 3
- [4] Tom Brown, Benjamin Mann, Nick Ryder, Melanie Subbiah, Jared D Kaplan, Prafulla Dhariwal, Arvind Neelakantan, Pranav Shyam, Girish Sastry, Amanda Askell, et al. Language models are few-shot learners. *Advances in neural information processing systems*, 33:1877–1901, 2020. 1, 3
- [5] Mingda Chen, Jingfei Du, Ramakanth Pasunuru, Todor Mihaylov, Srinii Iyer, Veselin Stoyanov, and Zornitsa Kozareva. Improving in-context few-shot learning via self-supervised training. In *Proceedings of the 2022 Conference of the North American Chapter of the Association for Computational Linguistics: Human Language Technologies*, pages 3558–3573, Seattle, United States, 2022. Association for Computational Linguistics. 3
- [6] Aakanksha Chowdhery, Sharan Narang, Jacob Devlin, Maarten Bosma, Gaurav Mishra, Adam Roberts, Paul Barham, Hyung Won Chung, Charles Sutton, Sebastian Gehrmann, et al. Palm: Scaling language modeling with pathways. *arXiv preprint arXiv:2204.02311*, 2022. 1
- [7] Hyung Won Chung, Le Hou, Shayne Longpre, Barret Zoph, Yi Tay, William Fedus, Yunxuan Li, Xuezhi Wang, Mostafa Dehghani, Siddhartha Brahma, et al. Scaling instruction-finetuned language models. *arXiv preprint arXiv:2210.11416*, 2022. 1
- [8] Qingxiu Dong, Lei Li, Damai Dai, Ce Zheng, Zhiyong Wu, Baobao Chang, Xu Sun, Jingjing Xu, and Zhifang Sui. A survey for in-context learning. *arXiv preprint arXiv:2301.00234*, 2022. 1
- [9] Tianyu Gao, Adam Fisch, and Danqi Chen. Making pre-trained language models better few-shot learners. *arXiv preprint arXiv:2012.15723*, 2020. 1, 3
- [10] Yash Goyal, Tejas Khot, Douglas Summers-Stay, Dhruv Batra, and Devi Parikh. Making the V in VQA matter: Elevating the role of image understanding in Visual Question Answering. In *Conference on Computer Vision and Pattern Recognition (CVPR)*, 2017. 5
- [11] Sawan Kumar and Partha Talukdar. Reordering examples helps during priming-based few-shot learning. In *Findings of the Association for Computational Linguistics: ACL-IJCNLP 2021*, pages 4507–4518, Online, 2021. Association for Computational Linguistics. 1, 3
- [12] Itay Levy, Ben Bogin, and Jonathan Berant. Diverse demonstrations improve in-context compositional generalization. *arXiv preprint arXiv:2212.06800*, 2022. 7
- [13] Bo Li, Yuanhan Zhang, Liangyu Chen, Jinghao Wang, Jingkang Yang, and Ziwei Liu. Otter: A multi-modal model with in-context instruction tuning. *arXiv preprint arXiv:2305.03726*, 2023. 3
- [14] Xiaonan Li and Xipeng Qiu. Finding supporting examples for in-context learning. *arXiv preprint arXiv:2302.13539*, 2023. 3
- [15] Xiaonan Li, Kai Lv, Hang Yan, Tianyang Lin, Wei Zhu, Yuan Ni, Guotong Xie, Xiaoling Wang, and Xipeng Qiu. Unified demonstration retriever for in-context learning. *arXiv preprint arXiv:2305.04320*, 2023. 3
- [16] Tsung-Yi Lin, Michael Maire, Serge Belongie, James Hays, Pietro Perona, Deva Ramanan, Piotr Dollár, and C Lawrence Zitnick. Microsoft coco: Common objects in context. In *Computer Vision—ECCV 2014: 13th European Conference, Zurich, Switzerland, September 6–12, 2014, Proceedings, Part V 13*, pages 740–755. Springer, 2014. 3, 4, 5
- [17] Haotian Liu, Chunyuan Li, Qingyang Wu, and Yong Jae Lee. Visual instruction tuning. In *NeurIPS*, 2023. 3
- [18] Jiachang Liu, Dinghan Shen, Yizhe Zhang, Bill Dolan, Lawrence Carin, and Weizhu Chen. What makes good in-context examples for GPT-3? In *Proceedings of Deep Learning Inside Out (DeeLIO 2022): The 3rd Workshop on Knowledge Extraction and Integration for Deep Learning Architectures*, pages 100–114, Dublin, Ireland and Online, 2022. Association for Computational Linguistics. 1, 3, 5
- [19] Ilya Loshchilov and Frank Hutter. Decoupled weight decay regularization. *arXiv preprint arXiv:1711.05101*, 2017. 5, 1
- [20] Yao Lu, Max Bartolo, Alastair Moore, Sebastian Riedel, and Pontus Stenetorp. Fantastically ordered prompts and where to find them: Overcoming few-shot prompt order sensitivity. In *Proceedings of the 60th Annual Meeting of the Association for Computational Linguistics*, 2022. 1

- ciation for Computational Linguistics (Volume 1: Long Papers), pages 8086–8098, Dublin, Ireland, 2022. Association for Computational Linguistics. 1, 2, 3
- [21] Sewon Min, Mike Lewis, Luke Zettlemoyer, and Hannaneh Hajishirzi. Metaicl: Learning to learn in context. In *Proceedings of the 2022 Conference of the North American Chapter of the Association for Computational Linguistics: Human Language Technologies*, pages 2791–2809, 2022. 1
- [22] Tai Nguyen and Eric Wong. In-context example selection with influences. *arXiv preprint arXiv:2302.11042*, 2023. 3
- [23] Feng Nie, Meixi Chen, Zhirui Zhang, and Xu Cheng. Improving few-shot performance of language models via nearest neighbor calibration. *arXiv preprint arXiv:2212.02216*, 2022. 1, 3
- [24] Alec Radford, Jeffrey Wu, Rewon Child, David Luan, Dario Amodei, Ilya Sutskever, et al. Language models are unsupervised multitask learners. 2019. 3
- [25] Alec Radford, Jong Wook Kim, Chris Hallacy, Aditya Ramesh, Gabriel Goh, Sandhini Agarwal, Girish Sastry, Amanda Askell, Pamela Mishkin, Jack Clark, et al. Learning transferable visual models from natural language supervision. In *International conference on machine learning*, pages 8748–8763. PMLR, 2021. 4
- [26] Ohad Rubin, Jonathan Herzig, and Jonathan Berant. Learning to retrieve prompts for in-context learning. *arXiv preprint arXiv:2112.08633*, 2021. 3
- [27] Haşim Sak, Andrew Senior, and Françoise Beaufays. Long short-term memory based recurrent neural network architectures for large vocabulary speech recognition. *arXiv preprint arXiv:1402.1128*, 2014. 5, 7
- [28] Hongjin Su, Jungo Kasai, Chen Henry Wu, Weijia Shi, Tianlu Wang, Jiayi Xin, Rui Zhang, Mari Ostendorf, Luke Zettlemoyer, Noah A Smith, et al. Selective annotation makes language models better few-shot learners. *arXiv preprint arXiv:2209.01975*, 2022. 1
- [29] Yu Sun, Shuohuan Wang, Shikun Feng, Siyu Ding, Chao Pang, Junyuan Shang, Jiaxiang Liu, Xuyi Chen, Yanbin Zhao, Yuxiang Lu, et al. Ernie 3.0: Large-scale knowledge enhanced pre-training for language understanding and generation. *arXiv preprint arXiv:2107.02137*, 2021. 3
- [30] Eshaan Tanwar, Manish Borthakur, Subhabrata Dutta, and Tanmoy Chakraborty. Multilingual llms are better cross-lingual in-context learners with alignment. *arXiv preprint arXiv:2305.05940*, 2023. 1
- [31] MosaicML NLP Team. Introducing mpt-7b: A new standard for open-source, commercially usable llms, 2023. Accessed: 2023-05-05. 3
- [32] Hugo Touvron, Thibaut Lavril, Gautier Izacard, Xavier Martinet, Marie-Anne Lachaux, Timothée Lacroix, Baptiste Rozière, Naman Goyal, Eric Hambro, Faisal Azhar, et al. Llama: Open and efficient foundation language models. *arXiv preprint arXiv:2302.13971*, 2023. 1, 3
- [33] Maria Tsimpoukelli, Jacob L Menick, Serkan Cabi, SM Eslami, Oriol Vinyals, and Felix Hill. Multimodal few-shot learning with frozen language models. *Advances in Neural Information Processing Systems*, 34:200–212, 2021. 1, 3
- [34] Ashish Vaswani, Noam Shazeer, Niki Parmar, Jakob Uszkoreit, Llion Jones, Aidan N Gomez, Łukasz Kaiser, and Illia Polosukhin. Attention is all you need. *Advances in neural information processing systems*, 30, 2017. 4, 5
- [35] Ramakrishna Vedantam, C Lawrence Zitnick, and Devi Parikh. Cider: Consensus-based image description evaluation. In *Proceedings of the IEEE conference on computer vision and pattern recognition*, pages 4566–4575, 2015. 4
- [36] Liang Wang, Nan Yang, and Furu Wei. Learning to retrieve in-context examples for large language models. *arXiv preprint arXiv:2307.07164*, 2023. 3
- [37] Xinyi Wang, Wanrong Zhu, Michael Saxon, Mark Steyvers, and William Yang Wang. Large language models are latent variable models: Explaining and finding good demonstrations for in-context learning. In *Thirty-seventh Conference on Neural Information Processing Systems*, 2023. 3
- [38] Jason Wei, Yi Tay, Rishi Bommasani, Colin Raffel, Barret Zoph, Sebastian Borgeaud, Dani Yogatama, Maarten Bosma, Denny Zhou, Donald Metzler, et al. Emergent abilities of large language models. *arXiv preprint arXiv:2206.07682*, 2022. 1
- [39] Jerry Wei, Jason Wei, Yi Tay, Dustin Tran, Albert Webson, Yifeng Lu, Xinyun Chen, Hanxiao Liu, Da Huang, Denny Zhou, et al. Larger language models do in-context learning differently. *arXiv preprint arXiv:2303.03846*, 2023. 1
- [40] Zhiyong Wu, Yaoxiang Wang, Jiacheng Ye, and Lingpeng Kong. Self-adaptive in-context learning. *arXiv preprint arXiv:2212.10375*, 2022. 1, 3
- [41] Xu Yang, Yongliang Wu, Mingzhuo Yang, Haokun Chen, and Geng Xin. Exploring diverse in-context configurations for image captioning. *arXiv preprint arXiv:2305.14800*, 2023. 2, 3, 6
- [42] Jiacheng Ye, Zhiyong Wu, Jiangtao Feng, Tao Yu, and Lingpeng Kong. Compositional exemplars for in-context learning. *arXiv preprint arXiv:2302.05698*, 2023. 3
- [43] Qinghao Ye, Haiyang Xu, Guohai Xu, Jiabo Ye, Ming Yan, Yiyang Zhou, Junyang Wang, Anwen Hu, Pengcheng Shi, Yaya Shi, Chaoya Jiang, Chenliang Li, Yuanhong Xu, Hehong Chen, Junfeng Tian, Qian Qi, Ji Zhang, and Fei Huang. mplug-owl: Modularization empowers large language models with multimodality, 2023. 3
- [44] Aohan Zeng, Xiao Liu, Zhengxiao Du, Zihan Wang, Hanyu Lai, Ming Ding, Zhuoyi Yang, Yifan Xu, Wendi Zheng, Xiao Xia, et al. Glm-130b: An open bilingual pre-trained model. *arXiv preprint arXiv:2210.02414*, 2022. 1
- [45] Susan Zhang, Stephen Roller, Naman Goyal, Mikel Artetxe, Moya Chen, Shuohui Chen, Christopher Dewan, Mona Diab, Xian Li, Xi Victoria Lin, et al. Opt: Open pre-trained transformer language models. *arXiv preprint arXiv:2205.01068*, 2022. 1
- [46] Yiming Zhang, Shi Feng, and Chenhao Tan. Active example selection for in-context learning. *arXiv preprint arXiv:2211.04486*, 2022. 3
- [47] Haozhe Zhao, Zefan Cai, Shuzheng Si, Xiaojian Ma, Kaikai An, Liang Chen, Zixuan Liu, Sheng Wang, Wenjuan Han, and Baobao Chang. Mmicl: Empowering vision-language model with multi-modal in-context learning. *arXiv preprint arXiv:2309.07915*, 2023. 1
- [48] Denny Zhou, Nathanael Schärli, Le Hou, Jason Wei, Nathan Scales, Xuezhi Wang, Dale Schuurmans, Claire Cui, Olivier

Bousquet, Quoc Le, et al. Least-to-most prompting enables complex reasoning in large language models. *arXiv preprint arXiv:2205.10625*, 2022. [1](#), [3](#)

- [49] Deyao Zhu, Jun Chen, Xiaoqian Shen, Xiang Li, and Mohamed Elhoseiny. Minigt-4: Enhancing vision-language understanding with advanced large language models. *arXiv preprint arXiv:2304.10592*, 2023. [3](#)

ICD-LM: Configuring Vision-Language In-Context Demonstrations by Language Modeling

Supplementary Material

Implementation Details. We provide additional implementation details for each experiment in Table 10. For all experiments, the batch size is set to 64, the warmup steps to 5% of total training steps, the scheduler as a cosine scheduler, and the optimizer as AdamW [19].

Table 10. Different settings of ICD-LM experiments, where the n is the number of anchor samples in \mathcal{A} , b is the beam size, and l is the length of ICD configurations.

		Training Parameters				$\mathcal{D}_{\mathcal{M}}$ Parameters			Avg:1~8
		lr	epoch	Freeze	Adapter	n	b	l	
IC	2-shot $\mathcal{D}_{\mathcal{M}}$	1.0×10^{-4}	20	✓	✓	5000	5	2	92.45
	4-shot $\mathcal{D}_{\mathcal{M}}$	1.0×10^{-4}	20	✓	✓	10000	10	4	90.88
	ICD-LM(LSTM)	1.0×10^{-3}	20	✓	✓	5000	5	2	92.12
	CIDEr Scorer	1.0×10^{-4}	20	✓	✓	5000	5	2	91.65
	Fixed Set-1	5.0×10^{-3}	10	✗	✗	5000	5	2	92.22
	Fixed Set-2	1.0×10^{-3}	20	✗	✗	5000	5	2	96.82
VQA	2-shot $\mathcal{D}_{\mathcal{M}}$	1.0×10^{-4}	20	✗	✗	5000	5	2	51.31
	4-shot $\mathcal{D}_{\mathcal{M}}$	1.0×10^{-4}	20	✗	✗	10000	10	4	49.61
	ICD-LM(LSTM)	1.0×10^{-5}	30	✗	✗	5000	5	2	49.32
	Fixed Set-1	1.0×10^{-3}	20	✗	✗	5000	5	2	50.93
	Fixed Set-2	1.0×10^{-3}	10	✗	✗	5000	5	2	47.80

Fixed Set ICD Configurations. We present four ICD configurations of the Fixed Set. Figure 5 displays two ICD configurations for IC, and Figure 6 displays the other two ICD configurations for VQA.



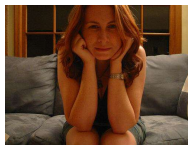
Caption: A one propeller airplane is in an airplane hanger.



Caption: A man skate boarding in a pool with another man looking on.



Caption: A large white polar bear swimming in a water tank.



Caption: A woman sitting on a couch with her hands to her head.



Caption: A black and white image a man on his phone and a toddler.



Caption: A dinner plate has a lot of different food on it.



Caption: This is a toilet with a black top.



Caption: The bowl has a half a grapefruit and the plate has donut and the other half.



Caption: A man riding a wave on top of a surfboard.



Caption: a white car sitting next to a pay here station.



Caption: a carousel horse has a rose in its mane.



Caption: a pizza with sauce, cheese and sausage sitting on a table.



Caption: A couple of ships sitting in the middle of a body of water.



Caption: Boats floating close together in a calm body of water.



Caption: A hand carved vase sitting on a blue cloth.



Caption: A black tray holding a big cheese pizza.

Fixed Set-1: IC

Fixed Set-2: IC

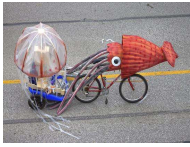
Figure 5. 8-shot ICD configurations Visualizations of IC Fixed Set.



Q: How many different types of vehicles are shown?
A: 1



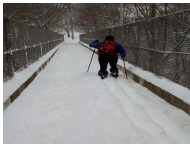
Q: What is the man wearing over his shirt?
A: vest



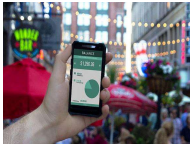
Q: What orange item is on the floor?
A: squid



Q: Is there a ramp in the picture?
A: no



Q: What is on the person's back?
A: backpack



Q: Does the word "balance" in the photo refer to a scale?
A: no



Q: What color is the bird standing on?
A: red



Q: What is in the background?
A: sun



Q: What is the girl holding on to
A: kite



Q: What hand is the tennis player holding the racket?
A: right



Q: What is on the person's arm?
A: shirt



Q: Is the elephant being bath?
A: no



Q: Are they in the woods?
A: yes



Q: What color is the room's walls?
A: white



Q: What color is the thing the man is sitting on?
A: blue



Q: What color are the trees?
A: green

Fixed Set-1: VQA

Fixed Set-2: VQA

Figure 6. 8-shot ICD configurations Visualizations of VQA Fixed Set.